

UC San Diego

UC San Diego Previously Published Works

Title

Anti-Inflammatory Effects and Joint Protection in Collagen-Induced Arthritis after Treatment with IQ-1S, a Selective c-Jun N-Terminal Kinase Inhibitor

Permalink

<https://escholarship.org/uc/item/06t4414w>

Journal

Journal of Pharmacology and Experimental Therapeutics, 353(3)

ISSN

0022-3565

Authors

Schepetkin, Igor A
Kirpotina, Liliya N
Hammaker, Deepa
et al.

Publication Date

2015-06-01

DOI

10.1124/jpet.114.220251

Peer reviewed

Anti-Inflammatory Effects and Joint Protection in Collagen-Induced Arthritis after Treatment with IQ-1S, a Selective c-Jun N-Terminal Kinase Inhibitor

Igor A. Schepetkin, Liliya N. Kirpotina, Deepa Hammaker, Irina Kochetkova, Andrei I. Khlebnikov, Sergey A. Lyakhov, Gary S. Firestein, and Mark T. Quinn

Department of Microbiology and Immunology, Montana State University, Bozeman, Montana (I.A.S., L.N.K., I.K., M.T.Q.); Division of Rheumatology, Allergy, and Immunology, University of California, San Diego School of Medicine, La Jolla, California (D.H., G.S.F.); Department of Chemistry, Altai State Technical University, Barnaul, Russia (A.I.K.); Department of Biotechnology and Organic Chemistry, Tomsk Polytechnic University, Tomsk, Russia (A.I.K.); and A.V. Bogatsky Physico-Chemical Institute, National Academy of Sciences of Ukraine, Odessa, Ukraine (S.A.L.)

Received November 11, 2014; accepted March 17, 2015

ABSTRACT

c-Jun N-terminal kinases (JNKs) participate in many physiologic and pathologic processes, including inflammatory diseases. We recently synthesized the sodium salt of IQ-1S (11*H*-indeno[1,2-*b*]quinoxalin-11-one oxime) and demonstrated that it is a high-affinity JNK inhibitor and inhibits murine delayed-type hypersensitivity. Here we show that IQ-1S is highly specific for JNK and that its neutral form is the most abundant species at physiologic pH. Molecular docking of the IQ-1S *syn* isomer into the JNK1 binding site gave the best pose, which corresponded to the position of cocrystallized JNK inhibitor SP600125 (1,9-pyrazoloanthrone). Evaluation of the therapeutic potential of IQ-1S showed that it inhibited matrix metalloproteinase 1 and 3 gene expression induced by interleukin-1 β in human fibroblast-like synoviocytes and significantly attenuated development of murine collagen-induced

arthritis (CIA). Treatment with IQ-1S either before or after induction of CIA resulted in decreased clinical scores, and joint sections from IQ-1S-treated CIA mice exhibited only mild signs of inflammation and minimal cartilage loss compared with those from control mice. Collagen II-specific antibody responses were also reduced by IQ-1S treatment. By contrast, the inactive ketone derivative 11*H*-indeno[1,2-*b*]quinoxalin-11-one had no effect on CIA clinical scores or collagen II-specific antibody titers. IQ-1S treatment also suppressed proinflammatory cytokine and chemokine levels in joints and lymph node cells. Finally, treatment with IQ-1S increased the number of Foxp3⁺CD4⁺CD25⁺ regulatory T cells in lymph nodes. Thus, IQ-1S can reduce inflammation and cartilage loss associated with CIA and can serve as a small-molecule modulator for mechanistic studies of JNK function in rheumatoid arthritis.

Introduction

Rheumatoid arthritis (RA) is a chronic and systemic destructive autoimmune disorder characterized by inflammation and progressive destruction of distal joints (Firestein, 2003). RA

leads to loss of mobility and joint function if not adequately treated. Because RA is an autoimmune and bone/cartilage degenerative disease, ideal therapies should combine immunomodulatory, anti-inflammatory, and anti-bone resorption properties. In recent years, substantial efforts have been focused on the development of novel synthetic small-molecule compounds that could disrupt the continued recruitment of inflammatory cells to the synovium and thereby limit the amount of destructive enzymes and proinflammatory cytokines in the local joint environment. Indeed, small-molecule compounds targeting kinase proteins are emerging as potential treatments for RA because multiple signaling kinases are involved in the pathogenesis of RA, and such inhibitors can be designed to recognize particular

This research was supported in part by the National Institutes of Health National Institute of General Medical Sciences IDeA Program [Grant P30-GM110732 (to M.T.Q.)]; the National Institutes of Health National Institute of Arthritis and Musculoskeletal and Skin Diseases [Grant R01-AR47825 (to G.S.F.)]; an equipment grant from the M.J. Murdock Charitable Trust; a US Department of Agriculture National Institute of Food and Agriculture Hatch project; and the Montana State University Agricultural Experiment Station.

I.A.S. and L.N.K. contributed equally to this work.

dx.doi.org/10.1124/jpet.114.220251.

ABBREVIATIONS: Ab, antibody; B220, 2,3-dimethyl-6(2-dimethylaminoethyl)-6*H*-indolo-(2,3-*b*)quinoxaline; BMS-345541, 4-(2'-aminoethyl)amino-1,8-dimethylimidazo[1,2-*a*]quinoxaline; Btk, Bruton's tyrosine kinase; CIA, collagen-induced arthritis; CII, type II collagen; DMEM, Dulbecco's modified Eagle's medium; DMSO, dimethylsulfoxide; ELISA, enzyme-linked immunosorbent assay; FBS, fetal bovine serum; FLS, fibroblast-like synoviocyte; FR167653, 1-(7-(4-fluorophenyl)-1,2,3,4-tetrahydro-8-(4-pyridyl)pyrazolo[5,1-*c*](1,2,4)triazin-2-yl)-2-phenylethanedione sulfate monohydrate; GM-CSF, granulocyte-macrophage colony-stimulating factor; GSK, glycogen synthase kinase; IFN, interferon; IKK, I κ B kinase; IL, interleukin; IQ-1, 11*H*-indeno[1,2-*b*]quinoxalin-11-one oxime; IQ-1S, 11*H*-indeno[1,2-*b*]quinoxalin-11-one oxime sodium salt; IQ-18, 11*H*-indeno[1,2-*b*]quinoxalin-11-one; JAK, Janus kinase; JNK, c-Jun N-terminal kinase; LN, lymph node; MAPK, mitogen-activated protein kinase; MCP-1, monocyte chemoattractant protein 1; MKK, MAP kinase kinase; MMP, matrix metalloproteinase; MVD, Molegro Virtual Docker; RA, rheumatoid arthritis; Rabeximod, 9-chloro-2,3-dimethyl-6-(*N,N*-dimethylaminoethylamino-2-oxoethyl)-6*H*-indolo[2,3-*b*]quinoxaline; SP600125, 1,9-pyrazoloanthrone; TNF, tumor necrosis factor; TPCA-1, 2-[(aminocarbonyl)amino]-5-(4-fluorophenyl)-3-thiophenecarboxamide; Treg, regulatory T cell.

conformations of their targets (Pesu et al., 2008; Cohen and Fleischmann, 2010; Kytтары, 2012; Meier and McInnes, 2014). For example, inhibitors of I κ B kinase (IKK)-2, glycogen synthase kinase (GSK)-3 β , c-Fms tyrosine kinase, spleen tyrosine kinase, Bruton's tyrosine kinase (Btk), phosphatidylinositol-3 kinases, and Janus kinases (JAKs) have been reported to be efficacious in animal models of RA (Podolin et al., 2005; Cuzzocrea et al., 2006; Toyama et al., 2010; Dehlin et al., 2011; Coffey et al., 2012; Xu et al., 2012).

Mitogen-activated protein kinases (MAPKs), including p38 MAPK, extracellular signal-regulated kinase, and c-Jun N-terminal kinase (JNK), are highly activated in the rheumatoid synovium and potentially contribute to destructive and inflammatory mechanisms that provide the rationale for targeting these pathways for drug discovery (Manning and Davis, 2003; Thalhamer et al., 2008; Guma and Firestein, 2012; Lee et al., 2012). Although inhibitors of p38 MAPK and extracellular signal-regulated kinase had beneficial effects in animal models of RA (Ohuri et al., 2007; Triantaphyllopoulos et al., 2010), studies on the efficacy of JNK inhibitors in these models are limited. Three distinct JNKs, designated as JNK1, JNK2, and JNK3, have been identified, and at least 10 different splicing isoforms exist in mammalian cells (Gupta et al., 1996; Rincón and Davis, 2009). JNK1 and JNK2 are widely expressed, whereas JNK3 is predominantly restricted to the brain, testis, and myocardium (Bogoyevitch et al., 2004). JNKs play important roles in regulating cytokine production and extracellular matrix degradation by matrix metalloproteinases (MMPs), and administration of JNK inhibitor SP600125 (1,9-pyrazoloanthrone) modestly decreased rat paw swelling in adjuvant-induced arthritis (Han et al., 2001). The individual roles of JNK1 and JNK2 in the pathogenesis of RA have not yet been fully determined. JNK1 has been implicated as a pivotal regulator of synovial inflammation in murine arthritis due to its role in mast cell degranulation and macrophage migration (Guma et al., 2010, 2011). However, JNK1 is not essential for inflammatory arthritis in transgenic mice (Köller et al., 2005), suggesting that signaling through JNK2 might compensate for JNK1 deficiency. Because the inhibition of both JNK1 and JNK2 isoforms would likely have a beneficial antiarthritic effect, it has been suggested that pan-JNK inhibitors may represent promising therapeutic agents for treatment of RA (Bogoyevitch et al., 2010; Koch et al., 2015).

We recently identified IQ-1 (11*H*-indeno[1,2-*b*]quinoxalin-11-one oxime) using high-throughput screening and demonstrated that this compound and its oxime analogs inhibited JNK enzymatic activity and, consequently, proinflammatory cytokine production by different murine and human cell systems (Schepetkin et al., 2012). In this study, we investigated the effect of the IQ-1S (11*H*-indeno[1,2-*b*]quinoxalin-11-one oxime sodium salt) on mouse collagen-induced arthritis (CIA), a common animal model of RA. Our findings demonstrate that IQ-1S significantly reduced the clinical severity of CIA and inhibited cartilage and bone destruction. The clinical effect was associated with attenuated serum titer of collagen II (CII)-specific antibodies (Abs) and suppression of proinflammatory cytokine expression in joint tissue and lymph node (LN) cells. Administration of IQ-1S dose-dependently increased the number of Foxp3⁺ CD4⁺ CD25⁺ regulatory T cells (Tregs) in LNs. Together, these results indicate that IQ-1S and related JNK inhibitors have therapeutic potential in the treatment of RA.

Materials and Methods

Compounds. JNK inhibitor IQ-1S was synthesized as previously described (Schepetkin et al., 2012). Ketone derivative 11*H*-indeno[1,2-*b*]quinoxalin-11-one (compound IQ-18; compound designation as in our previous publication; Schepetkin et al., 2012) was purchased from Sigma-Aldrich (St. Louis, MO). For in vitro studies, IQ-1S was dissolved in dimethylsulfoxide (DMSO) and diluted into the desired buffer or culture media. For in vivo treatments, the compounds were suspended in sterile physiologic saline.

pK_a Determination. The equilibrium pK_a value for IQ-1S was obtained by spectrophotometry using the method of Albert and Serjeant (1984).

Molecular Modeling. A three-dimensional model of JNK1 containing cocrystallized ligand SP600125 (Heo et al., 2004) was downloaded from the Protein Data Bank (PDB ID 1UKI) and imported into the Molegro Virtual Docker (MVD) program (MVD 2010.4.2; Molegro ApS, Aarhus, Denmark). Using a "Detect Cavity" module of MVD with probe size 2 Å, we detected four potential areas in the protein where ligands could be docked. A major cavity of 154 Å³ contained cocrystallized molecule SP600125, whereas the other three cavities identified were ≤ 13 Å³ and were not considered for docking. A spherical search space was placed at the geometric center of the SP600125 ligand, which embraced the SP600125 molecule and main portion of the cavity. This 8-Å radius sphere was used to generate initial poses by MVD. The spherical search space included, at least partially, 21 residues of JNK1 (Ile32, Gly33, Ser34, Val40, Cys41, Ala42, Ala53, Lys55, Ile86, Met108, Glu109, Leu110, Met111, Asp112, Ala113, Asn114, Ser155, Asn156, Val158, Val159, and Leu168). Side chains of these residues were considered flexible with MVD parameters "Tolerance" and "Strength" set to 0.9 and 0.7, respectively.

Before docking, structures of oxime IQ-1S (*syn* and *anti* isomers) and Rabeximod (9-chloro-2,3-dimethyl-6-(*N,N*-dimethylaminoethylamino-2-oxoethyl)-6*H*-indolo[2,3-*b*]quinoxaline; OxyPharma, Stockholm, Sweden) were preoptimized by the semiempirical PM3 method using HyperChem 8.0 software (Hypercube, Inc., Gainesville, FL) and saved in Tripos MOL2 format (Tripos, L.P., St. Louis, MO). The structures were then imported into the MVD program with the options "create explicit hydrogens" and "detect flexible torsions in ligands" enabled and docked using the search space indicated above with the option "constrain poses to cavity" switched on. MolDock score functions were used with a 0.3-Å grid resolution. Thirty docking runs were performed for each molecule. The postprocessing option "optimize H-bonds" was applied after docking. Similar poses were clustered at a root-mean-square deviation threshold of 2 Å.

Kinase Profiling and K_d Determination. Kinase profiling for IQ-1S was performed by KINOMEscan (DiscoverRx, San Diego, CA) using a panel of 91 protein kinases, as previously described (Fabian et al., 2005; Karaman et al., 2008). In brief, kinases were produced and displayed on T7 phages or expressed in HEK-293 cells. Binding reactions were performed at room temperature for 1 hour, and the fraction of kinase not bound to test compound was determined by capture with an immobilized affinity ligand and quantified by quantitative polymerase chain reaction. The screening at a fixed concentration (10 μ M) of the compound was performed in duplicate. IQ-1S was submitted for dissociation constant (K_d) determination toward MAP kinase kinases MKK4 and MKK7 using the same platform. For dissociation constant K_d determination, a 12-point half-log dilution series (a maximum concentration of 100 μ M) was used.

Isolation of Fibroblast-Like Synoviocytes and Analysis of MMP Expression. This study was approved by the Institutional Review Board of University of California, San Diego School of Medicine (La Jolla, CA), and informed consent was obtained from all participants. Synovial tissue was obtained from patients with RA at the time of total joint replacement, as previously described (Alvaro-Gracia et al., 1990). The diagnosis of RA conformed to American College of Rheumatology 1987 revised criteria (Arnett et al., 1988). The synovium was minced and incubated with 0.5 mg/ml collagenase

type VIII (Sigma-Aldrich) in serum-free RPMI 1640 (Life Technologies, Grand Island, NY) for 2 hours at 37°C, filtered, extensively washed, and cultured in Dulbecco's modified Eagle's medium (DMEM) (Life Technologies) supplemented with 10% fetal bovine serum (FBS) (Gemini Bio Products, Calabasas, CA), penicillin, streptomycin, gentamicin, and glutamine in a humidified 5% CO₂ atmosphere. Cells were allowed to adhere overnight, nonadherent cells were removed, and adherent fibroblast-like synoviocyte (FLSs) were split at 1:3 when 70%–80% confluent. FLSs were used from passages 3 through 9, during which time they are a homogeneous population of cells (<1% CD11b positive, <1% phagocytic, and <1% FcγRII and FcγRIII receptor positive).

For MMP mRNA analysis, FLSs were plated in six-well plates and cultured until 80% confluence, and they were subsequently serum starved (0.1% FBS/DMEM) for 24 hours. The cells were treated with IQ-1S (4, 10, and 25 μM) or DMSO for 1 hour before interleukin (IL)-1β stimulation (2 ng/ml) for 6 hours. The mRNA was isolated and reverse transcribed to obtain cDNA. Quantitative real-time polymerase chain reaction was performed using primer probe sets for MMP1, MMP3, and glyceraldehyde 3-phosphate dehydrogenase (Life Technologies). Threshold cycle values were obtained and normalized to glyceraldehyde 3-phosphate dehydrogenase expression.

Western Blotting. Cultured FLSs (passage 4) were plated at 2 × 10⁵ cells in six-well plates overnight in DMEM supplemented with 10% FBS and synchronized for 24 hours in DMEM/0.1% FBS. The cells were pretreated for 1 hour with IQ-1S or DMSO and then incubated with 0.5 ng/ml IL-1 or medium for 15 minutes at 37°C. The cells were then washed once with ice-cold phosphate-buffered saline and lysed with modified radioimmunoprecipitation assay buffer [50 mM HEPES, pH 7.4, 150 mM NaCl, 1% Triton X-100, 10% glycerol, 2.5 mM MgCl₂, 1.0 mM EDTA, 20 mM β-glycerophosphate, 10 mM NaF, 1 mM Na₃VO₄, and Protease inhibitor cocktail (Roche, Indianapolis, IN)]. Protein concentration of the lysates was measured using a MicroBCA Assay kit (Pierce, Rockford, IL), and 40 μg lysate was subjected to 10% SDS-PAGE and Western blot analysis. Anti-phospho-c-Jun (Ser63) was purchased from Cell Signaling Technology (Danvers, MA), and anti-mouse β-actin was from Sigma-Aldrich.

CIA Induction, Treatment, and Clinical Evaluation. C57BL/6 male mice (aged 6–8 weeks) were obtained from Charles River Laboratories (Wilmington, MA). All animal experiments were performed in accordance with National Institutes of Health guidelines and were approved by the Institutional Animal Care and Use Committee at Montana State University.

To induce CIA in C57BL/6 mice, lyophilized chicken CII (Chondrex, Redmond, WA) was solubilized in 0.05 M acetic acid (2 mg/ml), and 100 μg of CII emulsified in complete Freund's adjuvant containing 4 mg/ml *Mycobacterium tuberculosis* (Chondrex) was injected s.c. in the tail (Kochetkova et al., 2010, 2014). Using this method, nearly 100% of mice consistently showed clinical symptoms by day 25. IQ-1S (JNK inhibitor), IQ-18 (analog of IQ-1S, inactive for JNK), or sterile saline solution were injected intraperitoneally daily beginning at days -1, 7, 14, or 25 relative to the CII challenge, as indicated, and continued until day 31 or 38 after the CII challenge. Mice were scored using a scale of 0–3 for each limb for a maximal total score of 12, as previously described (Kochetkova et al., 2010): 0, no signs of inflammation; 1, mild redness or swelling of single digits; 2, significant swelling of ankle or wrist with erythema; and 3, severe swelling and erythema of multiple joints.

Histopathology. Forty days after the CII challenge, animals were euthanized, and their limbs were fixed in 10% neutral buffered formalin and decalcified in 5% formic acid for 3–6 days. The joints were embedded in paraffin and cut at 8-μm sections. Hematoxylin and eosin and toluidine blue staining were performed for each sample. Histopathological scores for each joint were determined on a graded 0–3 scale similar to that previously described (Schramm et al., 2004): 0, no changes; 1, synovial hyperplasia and mild inflammatory infiltration; 2, pannus formation with cartilage degeneration; and 3, heavy inflammatory infiltration and debris in the joint, severe chondrocyte and cartilage matrix loss with new bone tissue substitution,

and bone destruction. Paw and knee joint scores were estimated, with a total maximum score of 18 possible per mouse. Cartilage degeneration was scored in toluidine blue-stained sections on a graded 0–3 scale, as previously described (Bernotiene et al., 2004): 0, no cartilage loss; 1, minimal chondrocytes and proteoglycan loss in the superficial zone; 2, moderate chondrocyte and proteoglycan loss into the middle zone but above the tidemark; and 3, severe cartilage degeneration through the tidemark.

Anti-CII Ab Enzyme-Linked Immunosorbent Assay. Serum samples from mice with CIA were collected on day 40 after the CII challenge, and samples of diluted sera were added to microtiter plates (Greiner Bio-One, Monroe, NC) coated with 2 μg/ml enzyme-linked immunosorbent assay (ELISA)-grade mouse CII (Chondrex). Horseradish peroxidase-conjugated goat anti-mouse total IgG, IgG₁, IgG_{2a}, IgG_{2b}, and IgG₃ (Southern Biotechnology Associates, Birmingham, AL) were used as detecting Abs. Reactions were developed with 2,2'-azino-bis(3-ethylbenzothiazoline-6-sulphonic acid (Moss Inc., Pasadena, MD), and absorbance was measured at 415 nm using a SpectraMax Plus microplate reader (Molecular Devices, Sunnyvale, CA). End point titer represents the reciprocal logarithm of two for the serum dilution with absorbance ≥0.1 above negative control.

Sample Preparation for Cytokine Assessment. One front and one rear paw from each mouse were removed, combined, and then homogenized in 1.0 ml/200 mg paw weight of lysis medium (RPMI 1640 containing 2 mM phenylmethylsulfonyl fluoride and 1 μg/ml final concentration of aprotinin, leupeptin, and pepstatin A; Sigma-Aldrich) (Tissi et al., 2009). The homogenized tissues were then centrifuged at 2000g for 10 minutes, and supernatants were filter sterilized (0.2 μm) and stored at -70°C until analyzed.

Upon termination of the study (day 40 after the CII challenge), axillary, inguinal, and popliteal LN mononuclear cells were purified and cultured (5 × 10⁶ cells/ml) alone or with 50 μg/ml CII for 3 days in a complete medium: RPMI 1640 medium supplemented with 10% of FBS (Invitrogen, Carlsbad, CA), 2 mM L-glutamine, 50 μM 2-mercaptoethanol (Sigma-Aldrich), 100 U/ml penicillin, 100 μg/ml streptomycin, 1 mM sodium pyruvate, and 0.1 mM nonessential amino acids (Kochetkova et al., 2008).

Cytokine ELISA. The levels of cytokines/chemokines, including tumor necrosis factor (TNF), granulocyte-macrophage colony-stimulating factor (GM-CSF), IL-1β, IL-6, IL-17, monocyte chemoattractant protein (MCP)-1, and interferon (IFN)-γ were measured in culture supernatants and homogenized paw tissues using ELISA kits (BD Biosciences, San Jose, CA) for mouse cytokines/chemokines.

Flow Cytometry. Upon termination of the disease course, LN cells were stained with fluorochrome-labeled anti-CD25 (BD Pharmingen, Franklin Lakes, NJ) and anti-CD4 monoclonal antibodies (eBioscience, San Diego, CA). For analysis of forkhead box p3 (Foxp3) intracellular expression, cells were further fixed in 2% paraformaldehyde, permeabilized with ice-cold methanol, and stained with fluorochrome-labeled anti-Foxp3 monoclonal Ab (eBioscience) or isotype control. Fluorescence was acquired on an LSR II flow cytometer (BD Biosciences, San Diego, CA) with BD FACSDiva software. All samples were analyzed using FlowJo software (Tree Star, Ashland, OR).

Statistical Analysis. The nonparametric Mann-Whitney *U* test was used for statistical analysis of CIA clinical scores, histology scores, and cartilage destruction. FLS data were analyzed by two-way analysis of variance with Tukey's multiple comparison test, and differences were considered statistically significant if *P* < 0.05. The *t* test and one-way analysis of variance were used for analysis of ELISA results and flow cytometry data. Results were considered statistically significant if *P* < 0.05.

Results

Characterization of IQ-1S Specificity. We previously reported that the binding affinities (*K_d*) of IQ-1S toward JNK1, JNK2, and JNK3 were 390, 360, and 87 nM, respectively (Schepetkin et al., 2012). However, a detailed kinase

inhibition profile for IQ-1S was not performed. Here, IQ-1S was profiled in a competition binding assay for its ability to compete with an active site-directed ligand for 91 different kinases. The screening revealed that IQ-1S is a highly specific inhibitor of human JNK isoforms compared with the other kinases tested (Fig. 1). Note that IQ-1S did not inhibit other kinases that represent potential targets for RA treatment, including GSK-3 (*GSK3B*), JAK2, JAK3, phosphatidylinositol-3 kinase (*PIK3C2B*, *PIK3CA*, and *PIK3CG*), Btk (*BTK*), IKK-2 (*IKKB*), Aurora kinases A and B (*AURKA* and *AURKB*), p21-activated kinase 1 (*PAK1*), and proviral integration site kinase 2 (*PIM2*) (Fig. 1). Because JNK is typically activated by MKK4 and MKK7 and both MKKs are phosphorylated in rheumatoid synovium (Sundarajan et al., 2003; Inoue et al., 2006), binding affinities of IQ-1S toward these kinases were also determined. However, IQ-1S demonstrated only a low binding affinity for MKK4 (K_d approximately 2.2 μ M) and there was no affinity for MKK7.

Molecular Modeling of IQ-1S in the JNK1 Binding Site. Since the protonation state can affect molecular charge and ligand binding affinity (Vinh et al., 2012), we determined which species was present at physiologic pH by measuring its pK_a and found it to be 8.9 ± 0.2 (data not shown). Thus, the neutral molecule is the most abundant form of IQ-1S at physiologic pH.

To better understand the interaction of IQ-1S with JNK, molecular docking studies were performed using the crystal structure of JNK1 (Dérillard et al., 1994; Wang et al., 2001). As with other oximes, the neutral molecule of IQ-1S can exist as *syn* and *anti* stereoisomers with presumably different biologic activities (Ogata et al., 1986). Docking of the *syn* isomer into the JNK1 binding site gave the best pose, which was almost identical to that of cocrystallized JNK inhibitor SP600125 (Fig. 2A). Importantly, the location of these molecules is close to JNK1 residues Met111 and Glu109, which is critical for the activity of JNK inhibitors (Heo et al., 2004; Lee et al., 2013). Docking of the oxime *anti* isomer revealed to a pose quite

different from that of the *syn* isomer and SP600125 (Fig. 2A), indicating that only the *syn* isomer is active. Because the IQ-1S structure is similar to Rabeximod, an anti-inflammatory compound (Hultqvist et al., 2009) with unknown molecular target(s), Rabeximod was also docked in the JNK1 binding site. We found that the plane of the Rabeximod heterocyclic moiety had an orientation quite different from that of SP600125 and IQ-1S (Fig. 2B) and was located far away from Met111 and Glu109. Thus, these data also suggest that JNK is likely not a target for Rabeximod.

IQ-1S Inhibits MMP Expression and c-Jun Phosphorylation in Rheumatoid FLSs. FLSs obtained by arthroplasty from tissue of patients with RA are an excellent in vitro model for screening novel compounds with antiarthritic potential (Bartok and Firestein, 2010; Rosengren et al., 2012). We evaluated whether IQ-1S altered *MMP1* and *MMP3* gene expression by IL-1 β -stimulated human FLSs and found that cells pretreated with IQ-1S exhibited a dose-dependent reduction in *MMP1/MMP3* mRNA levels compared with the vehicle-treated group (Fig. 3, A and B). We also confirmed that IQ-1S inhibited c-Jun phosphorylation in FLSs (Fig. 3C), which confirms our previous observation in human MonoMac-6 cells (Schepetkin et al., 2012). Together, these data suggest that IQ-1S may protect joints in part by decreasing *MMP1/MMP3* expression.

IQ-1S Suppresses CIA Severity. We previously determined that the serum IQ-1S concentration was $7.4 \mu\text{M} \times \text{h}^{-1}$ after intraperitoneal administration of 30 mg/kg IQ-1S in mice (Schepetkin et al., 2012). On the basis of these pharmacokinetic data and the observation that at least 4 μM IQ-1S was required for in vitro activity in the FLS assay, we used 30 mg/kg i.p. IQ-1S as a daily dose in most experiments for CIA treatment. To test the therapeutic potential of IQ-1S on CIA, treatment was initiated 1 day before induction of CIA. Mice treated intraperitoneally daily with 30 mg/kg IQ-1S displayed significant reductions in the severity of CIA compared with vehicle-treated mice, as assessed by the mean arthritis score

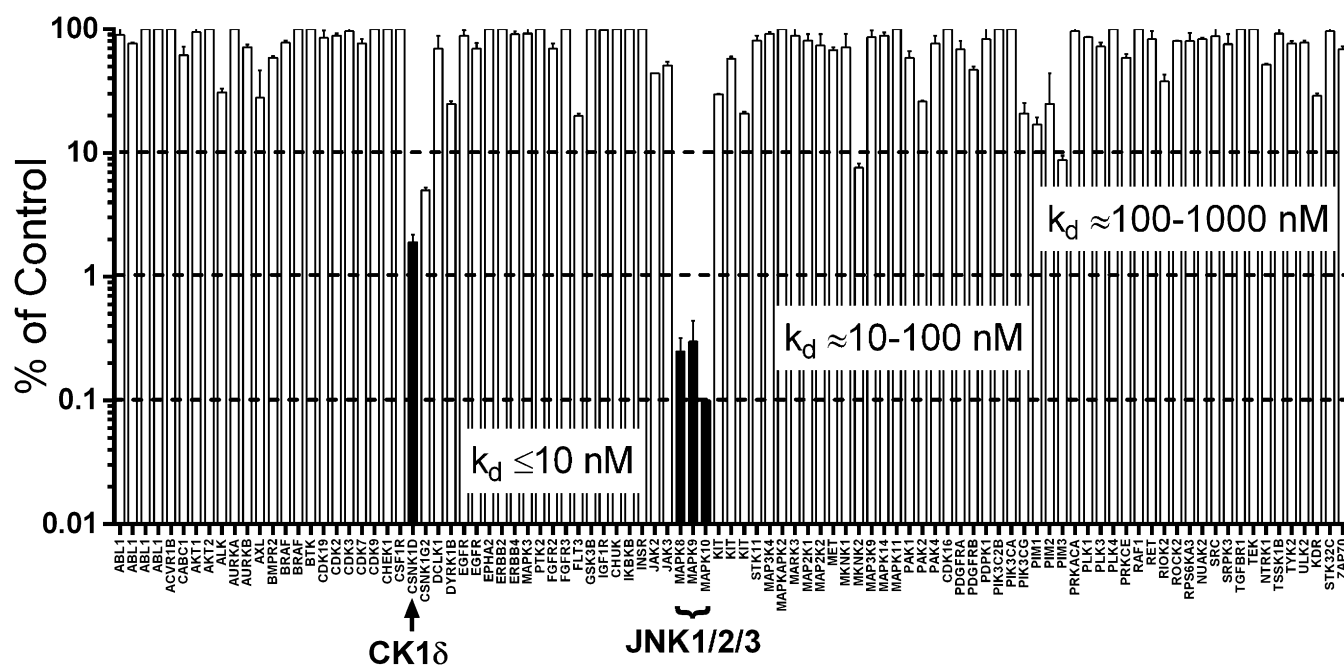


Fig. 1. Kinase profile of IQ-1S. Kinases were evaluated using the DiscoverX KINOMEScan platform. The percent inhibition of binding to an active site-directed ligand for each of the indicated kinases after treatment with 10 μ M IQ-1S is shown. The data are presented as the mean \pm S.D. of duplicate experiments.

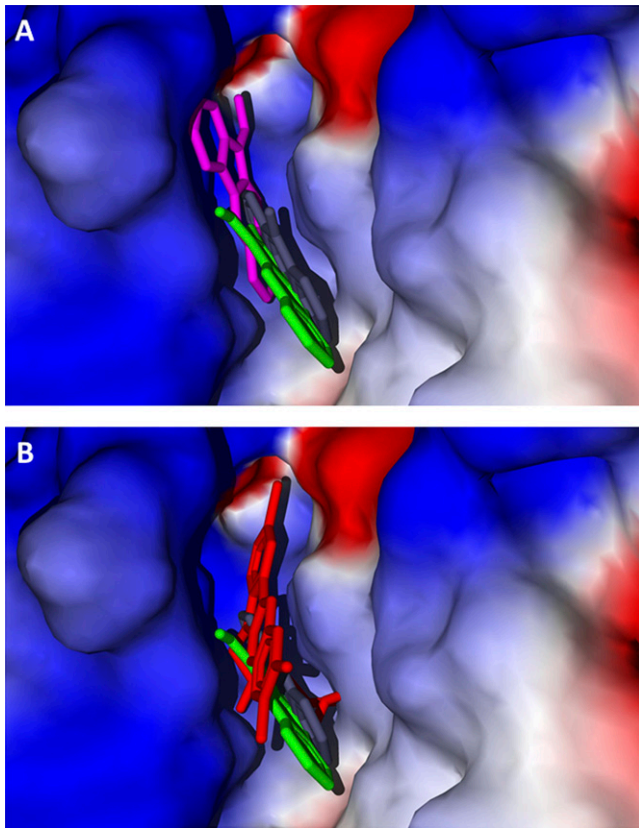


Fig. 2. Molecular docking of IQ-1S and Rabeximod in the JNK1 binding site. (A) The positions of the *syn* (green) and *anti* (magenta) isomers of the neutral form of IQ-1S as well as cocrystallized JNK inhibitor SP600125 (violet) in the JNK1 binding site are shown. (B) The positions of the *syn* isomer of the neutral form of IQ-1S (green), cocrystallized JNK inhibitor SP600125 (violet), and Rabeximod (red) in the JNK1 binding site are shown. The binding site region is shown by surface color according to electrostatic properties (red and blue represent negatively and positively charged areas, respectively).

(Fig. 4A). Although disease symptoms appear usually at day 21 postinduction, immune pathologic processes begin soon after CII injection (Brand et al., 2003), and initiation of administration of a test agent between days 0 and 21 after the CIA induction could be considered as a combined prevention/treatment model. Thus, starting at days 7 or 14 after the challenge with CII, the mice were treated intraperitoneally daily with IQ-1S (30 mg/kg). Remarkably, we observed that mice treated with IQ-1S at 1 or 2 weeks after disease induction also displayed significant reductions in CIA severity (Fig. 4A). Indeed, no significant difference was found in CIA severity between mice with preventive administration of IQ-1S (from day -1) and mice treated from day 7 or day 14 postchallenge.

We also evaluated the effects of IQ-1S on fully manifested arthritis. For these studies, mice with established CIA (average visual score of 2 at day 25 after CIA induction) were randomized and treated daily with 30 mg/kg IQ-1S or saline. We found that progression of established arthritis was also inhibited by IQ-1S treatment (Fig. 4B).

For determination of the optimal therapeutic dose of IQ-1S, the compound was administrated i.p. daily starting at day 7 after the CII challenge with 5, 20, 30, and 50 mg/kg doses. As shown in Fig. 4C, the mean clinical score of CIA was reduced in a dose-dependent manner. Both 30 and 50 mg/kg doses

were equally effective and significantly inhibited CIA more than the 20 mg/kg dose at the peak of the disease (33–37 days). Although the average mean clinical score was lower between 21 and 35 days at a 5 mg/kg dose, a significant reduction in disease severity was found only on 29 and 31 days at this dose.

As a control for compound specificity, we treated mice with IQ-18, an analog of IQ-1S that exhibited no JNK inhibitory activity (Schepetkin et al., 2012), and we found that it had no effect on CIA clinical scores (Fig. 4D).

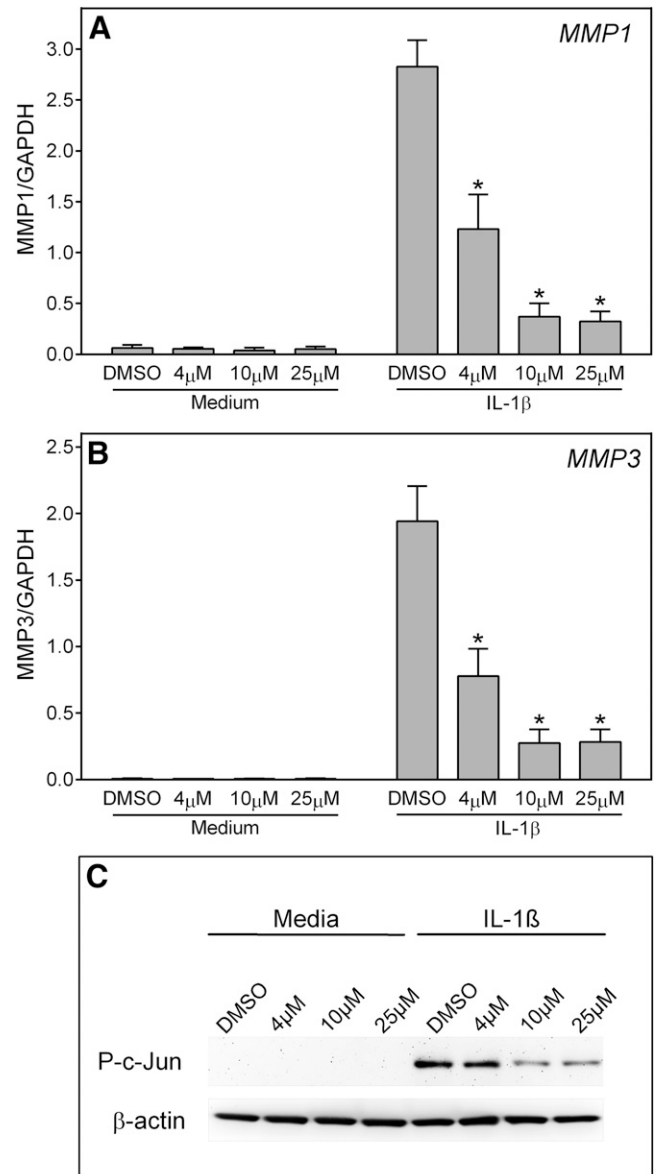


Fig. 3. IQ-1S decreases *MMP1* and *MMP3* gene expression and c-Jun phosphorylation in FLSs from RA patients. (A and B) FLSs were treated with DMSO or IQ-1S (4, 10, or 25 μM, as indicated) and stimulated with control medium or 2 ng/ml IL-1β for 6 hours. *MMP1* (A) and *MMP3* (B) gene expression was evaluated by quantitative polymerase chain reaction and normalized to glyceraldehyde 3-phosphate dehydrogenase (*GAPDH*), as described in *Materials and Methods*. The results are shown as mean ± S.E.M. of three different RA lines. **P* < 0.05 compared with DMSO control. (C) FLSs were pretreated for 1 hour with the indicated concentrations of IQ-1S or DMSO and then incubated with 0.5 ng/ml IL-1 or medium for 15 minutes at 37°C. Equal concentrations of cell lysates were separated by SDS-PAGE, followed by Western blotting for phospho-C-Jun (P-c-Jun) and β-actin, as described in *Materials and Methods*. Representative of two independent experiments.

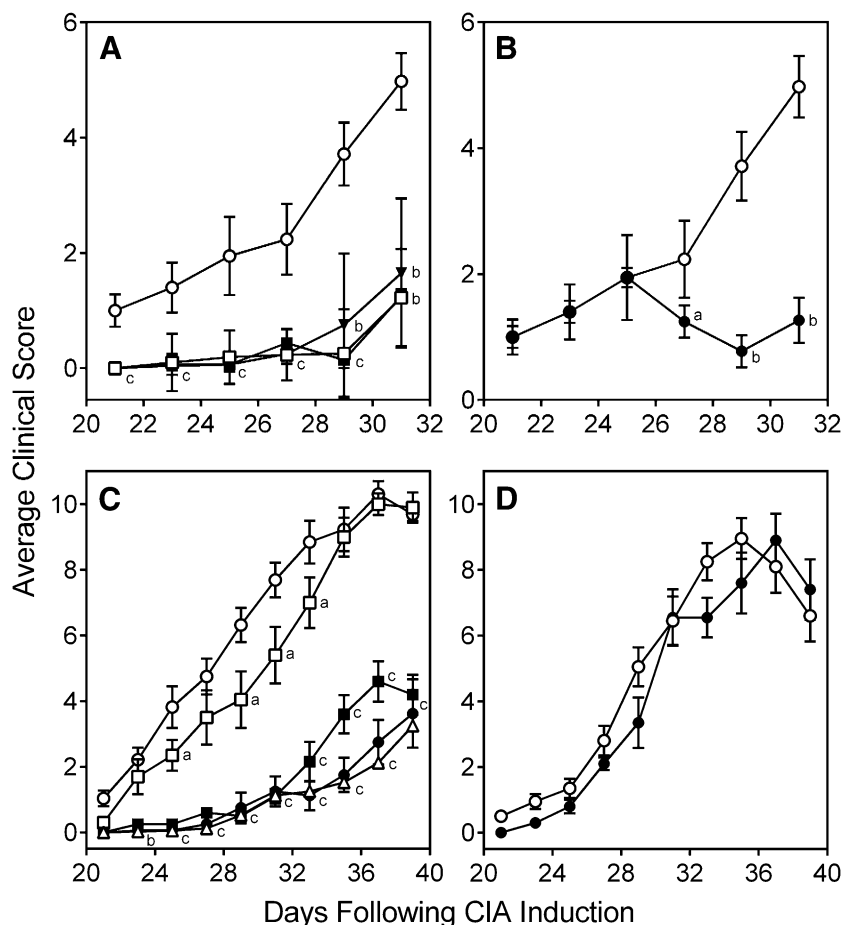


Fig. 4. JNK inhibitor IQ-1S prevents and treats CIA. (A) Mice were treated intraperitoneally daily with 30 mg/kg IQ-1S starting 1 day before induction of CIA (day -1) (□), 7 days after the CII challenge (■), and 14 days after the CII challenge (▼) until day 31, and clinical scores were determined as described in *Materials and Methods*. Control mice were treated intraperitoneally daily with sterile saline (○). (B) For CIA treatment, mice with established CIA (average score of 2 at day 25) were randomized and treated with control saline (○) or 30 mg/kg IQ-1S (●) until day 31, and clinical scores were determined. (C) Starting at day 7 after the CII challenge, mice were treated intraperitoneally daily with 5 (□), 20 (■), 30 (●), or 50 (△) mg/kg IQ-1S until day 38, and clinical scores were determined. Control mice were treated intraperitoneally daily with saline (○). (D) Starting at day 7 after the CII challenge, mice were treated intraperitoneally daily with control saline (○) or 30 mg/kg IQ-18 (●) until day 38, and clinical scores were determined. For each panel, results are shown as the mean of 10 mice per group \pm S.E.M. ^a $P < 0.05$; ^b $P < 0.01$; ^c $P < 0.001$ compared with saline control.

Histopathological analysis was performed on ankle joints harvested from mice with CIA receiving IQ-1S or saline, and representative images of hematoxylin and eosin- and toluidine blue-stained joint tissue are shown in Fig. 5A. Severe bone erosion, synovial hyperplasia, and infiltration of inflammatory cells were seen in the joints of saline-treated CIA mice. By contrast, there was little bone erosion, synovial hyperplasia, and cellular infiltration in IQ-1S-treated CIA mice. Furthermore, histologic scoring showed significant differences between IQ-1S-treated and control groups (Fig. 5B). Thus, consistent with the reductions in CIA clinical score, IQ-1S treatment clearly protected these mice from bone and cartilage destruction.

IQ-1S Decreases Serum Titer of CII-Specific Abs.

Injected CII-specific Abs can evoke transient arthritis, indicating that Ab responses play an important role in pathogenesis of CIA (Myers et al., 1997; Nandakumar et al., 2003). To determine the effect of IQ-1S on B cells in vivo, the levels of CII-specific Abs were measured in vehicle-treated or IQ-1S-treated CIA mice. We found that the titers of IgG, IgG₁, IgG_{2a}, and IgG₃ in the IQ-1S-treated group (doses 20 and 50 mg/kg) were significantly lower than those in the saline-treated group (Fig. 6). We also evaluated the titers of IgG, IgG₁, IgG_{2a}, and IgG₃ in IQ-18-treated CIA mice (30 mg/kg dose) and found that this inactive analog (Schepetkin et al., 2012) did not affect CII-specific Ab titers, which were not significantly different from vehicle control-treated CIA mice (data not shown).

IQ-1S Decreases Cytokine Levels in Paw Tissues and LN Cells.

The release of proinflammatory cytokines by macrophages

and other myeloid cells during RA causes cartilage damage and joint destruction (Schurgers et al., 2011; Zhou et al., 2011; Azizi et al., 2013). Since JNK has been shown to modulate cytokine expression in various in vitro and in vivo models (Rincón and Pedraza-Alva, 2003; Rincón and Davis, 2009; Guma and Firestein, 2012), we analyzed the effects of IQ-1S on expression of different cytokines and chemokines in paw homogenates isolated from control and IQ-1S-treated CIA mice, as well as naïve mice. Importantly, all of the seven proinflammatory cytokines/chemokines analyzed, including IL-1 β , IL-6, IL-17, IFN- γ , TNF, GM-CSF, and MCP-1, were significantly lower in IQ-1S-treated mice (20 and 50 mg/kg) versus control CIA mice (Fig. 7). Although IQ-1S had a dose-dependent effect on production of IL-1 β , IL-17, IL-6, IFN- γ , and TNF in joint tissue, the inhibitor was approximately equally active versus MCP-1 and GM-CSF at both doses tested.

JNK can potentially regulate T-cell development, proliferation, and cytokine production (Rincón and Pedraza-Alva, 2003; Rincón and Davis, 2009). To test whether IQ-1S suppressed the production of inflammatory cytokines/chemokines by CII-specific T cells, we assessed CII-induced cytokine production in vitro by LN cells isolated from treated and control mice. Equivalent numbers of cells from IQ-1S-treated and vehicle-treated CIA mice were cultured for 72 hours in the presence of CII. We found that the production of proinflammatory cytokines/chemokines IL-6, IL-17, TNF, IFN- γ , and MCP-1 were significantly lower in IQ-1S-treated mice (20 and 50 mg/kg) compared with control CIA mice (Fig. 8). The level of IL-1 β was

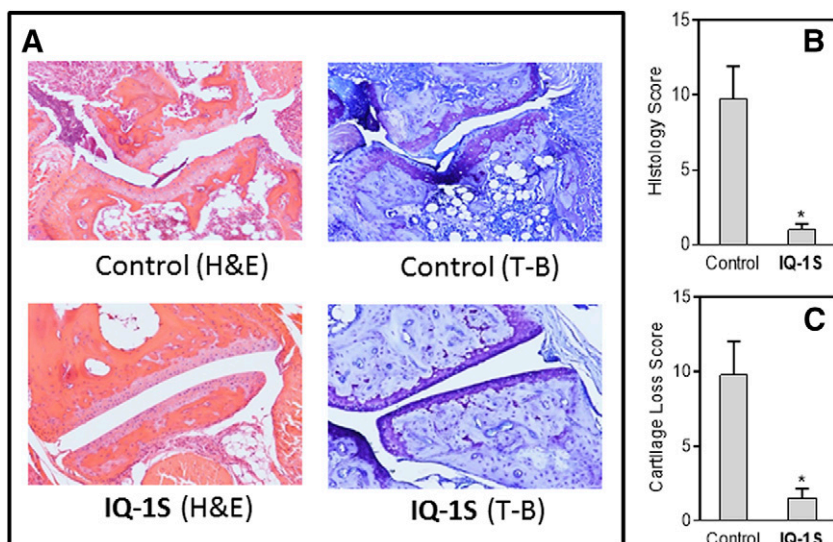


Fig. 5. Effect of IQ-1S on inflammation and cartilage loss in CIA mice. Starting at day 7 after the CII challenge, mice were treated intraperitoneally daily with 30 mg/kg IQ-1S in sterile saline until day 38, when the study ended. Control mice received saline alone. (A) H&E- and toluidine blue-stained knee sections. (B and C) Histology score (B) (0–3 per section) and cartilage loss (C) (0–3 per section) were graded for each limb and knee section. Total maximum scores of 18 were possible per mouse. The results show the mean of five mice per group \pm S.E.M. * $P < 0.01$ compared with saline control. T-B, toluidine blue.

significantly lower only in the 50 mg/kg treatment group, and there were no differences between levels of GM-CSF in treated and control CIA mice (Fig. 8).

IQ-1S Increases Number of Tregs. Tregs induce protection against CIA by diminishing joint inflammation (Carranza et al., 2012). Therefore, we evaluated the levels of Tregs in LNs isolated from CIA mice at day 40 and found that IQ-1S (20 and 30 mg/kg) treatment dose-dependently increased the number of CD4⁺ cells expressing CD25 and Foxp3 (Fig. 9).

Discussion

JNK plays a key role in both adaptive and innate immunity and therefore represents an excellent therapeutic target for directly treating and/or cotargeting in the treatment of inflammatory autoimmune diseases such as RA (Bogoyevitch et al., 2004, 2010; Mehan et al., 2011). A variety of small-molecule JNK inhibitors with anti-inflammatory properties have been reported to date (Bhagwat, 2007), but only few have been tested for the treatment of arthritis. Previous studies

showed that SP600125 treatment limited the development and progression of arthritis in animal models (Han et al., 2001, 2012); however, this compound is relatively nonspecific (Bain et al., 2003). By contrast, we show here that IQ-1S is quite specific for JNK versus all other off-target kinases tested and that it is an effective therapeutic that can reduce inflammation and cartilage loss associated with CIA.

To further understand the pharmacological features of IQ-1S and define the biologically active species, we performed molecular docking studies on the geometric isomers of IQ-1S and found that the *syn* isomer of this neutral molecule is the molecular species that binds to the JNK1 active site similarly to the position of cocrystallized JNK inhibitor SP600125, whereas the *anti* isomer did not bind in an orientation that would allow it to interact with JNK residues known to be important for inhibitory activity. Thus, the *syn* isomer of the neutral form or IQ-1S is most likely the active kinase inhibitor. In addition, these results suggest that the ratio of *syn* and *anti* isomers could be important in the preparation of IQ-1S or additional analogs. We are currently investigating this issue in efforts to define the ratio of these isomers in IQ-1S preparations.

We previously reported that IQ-1S had anti-inflammatory potential in vivo using a murine delayed-type hypersensitivity model (Schepetkin et al., 2012). Here, we evaluated the therapeutic potential of IQ-1S in RA using in vitro and in vivo approaches. We demonstrated that IL-1 β -induced *MMP1/MMP3* expression in rheumatoid FLSs was dose-dependently blocked by IQ-1S, supporting the conclusion that JNKs are targets of proinflammatory cytokine signaling. Thus, one aspect of the therapeutic effects observed for IQ-1S may be derived from its ability to target FLSs and potentially ameliorate their aggressive phenotype in RA. Indeed, the destruction of joint tissue seen in RA is due, in large part, to the aggressive phenotype of FLSs in the synovial intimal lining, because rheumatoid FLSs produce MMPs that contribute to destruction of extracellular matrix components within articular cartilage and cytokines that perpetuate inflammation (Burrage et al., 2006; Bartok and Firestein, 2010). Moreover, MMP-1 and MMP-3 are primary serum markers of RA that fluctuate with disease development and severity (Prince, 2005) and JNK plays a pivotal

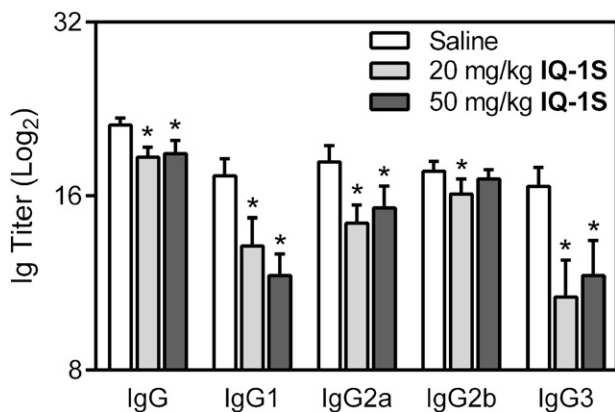


Fig. 6. Effect of IQ-1S on Ab response to CII. Starting at day 7 after the CII challenge, mice were treated intraperitoneally daily with saline, 20 mg/kg IQ-1S, or 50 mg/kg IQ-1S, as indicated, until day 38. Mice were euthanized, and sera were collected for measurement of IgG, IgG1, IgG2a, IgG2b, and IgG3 against CII. The results show the mean of 10 mice per group \pm S.D. * $P < 0.05$ compared with saline control.

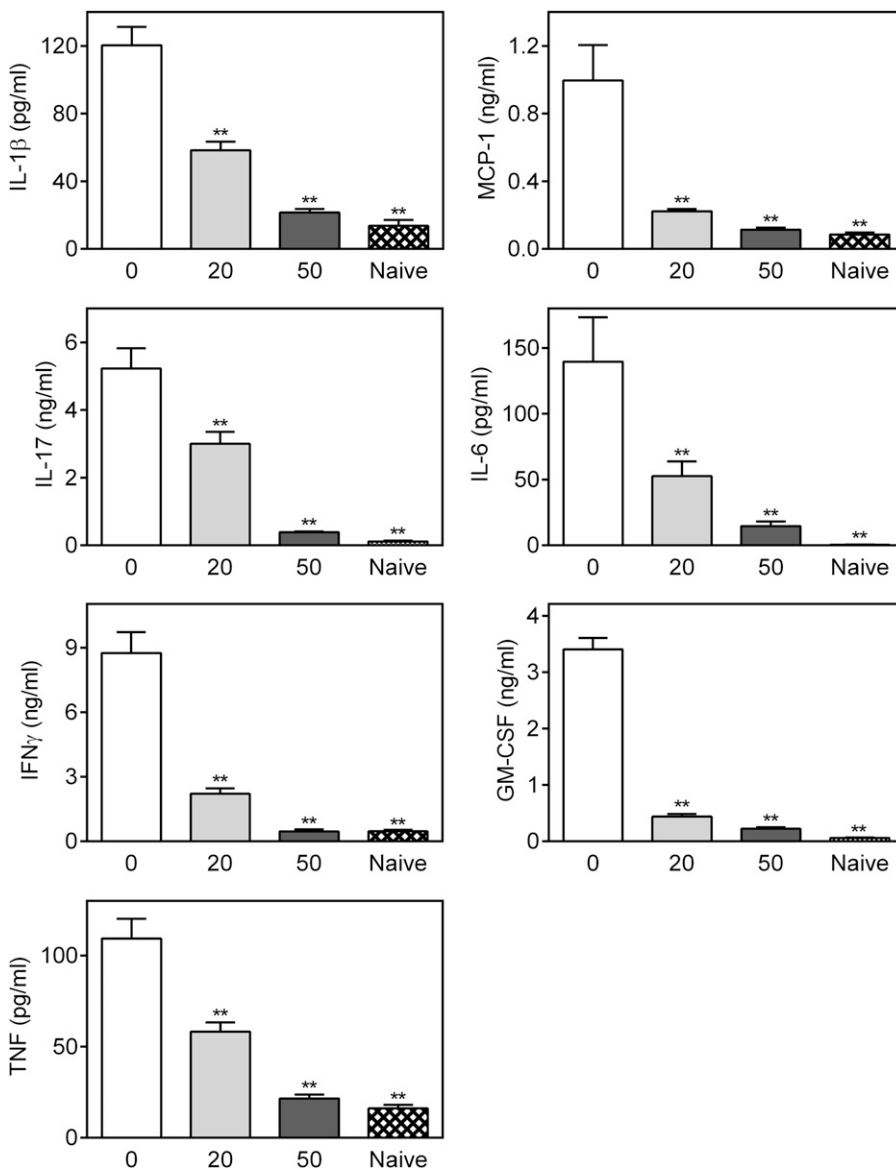


Fig. 7. IQ-1S suppresses inflammatory cytokines in paw homogenates from CIA mice. Starting at day 7 after the CII challenge, mice were treated intraperitoneally daily with saline (0), 20 mg/kg IQ-1S (20), or 50 mg/kg IQ-1S (50) until day 38. Mice were euthanized, and cytokines were quantified in paw homogenates by ELISA. Naive mice did not receive CII or IQ-1S. For each panel, the results show the mean of one experiment (three to four replicates) \pm S.D., which is representative of three independent experiments. ** $P < 0.01$ compared with saline control.

role in *MMP* gene expression in FLSs (Han et al., 1999; Liacini et al., 2002; Inoue et al., 2005).

CIA is a representative animal model of RA for evaluation of therapeutics (McIntyre et al., 2003; Nishikawa et al., 2003; Hegen et al., 2008). Our studies showed that treatment with IQ-1S inhibited the progression of CIA using both prophylactic (before onset of RA) and therapeutic (after RA onset) protocols. Furthermore, histopathological analyses confirmed the therapeutic potential of IQ-1S, because only mild signs of inflammation and minimal cartilage loss were found in treated mice. The development of CIA requires both adaptive and innate immune responses through production of CII-specific Abs and generation of CII-specific T cells (Brand et al., 2003). Thus, we tested serum titers of IgG, IgG₁, IgG_{2a}, and IgG₃ and found that IQ-1S suppressed the production of Abs to CII by B cells, especially of IgG₁ and IgG₃ subclasses. Since the production of anti-CII IgG₁ and IgG₃ represent T cell-dependent and -independent responses, respectively (Stevens et al., 1988), the therapeutic effect of IQ-1S on CIA could be associated with direct inhibition of B cell activity.

Indeed, JNK2 can regulate Ab production from B cells under some experimental conditions (Cao et al., 2010).

In an evaluation of the mechanisms contributing to the protection of joints from inflammatory damage, we found that tissue concentrations of proinflammatory cytokines and chemokines in paw homogenates were significantly lower in the CIA mice treated with IQ-1S, suggesting that IQ-1S suppressed systemic inflammation and joint destruction by inhibiting the local production of cytokines/chemokines. Because expression of MCP-1 and GM-CSF in the paw homogenates was effectively inhibited even at the lowest dose tested (20 mg/kg), IQ-1S could specifically be affecting macrophage maturation and activity. Consistent with the reduction in clinical scores and bone and cartilage destruction, LN levels of IL-1 β , IL-6, IL-17, TNF, IFN- γ , and MCP-1 were also significantly suppressed in IQ-1S-treated mice. These cytokines/chemokines play a central role in the pathogenesis of RA by recruiting and activating macrophages, neutrophils, and mast cells (Drexler et al., 2008; Guma et al., 2010). By contrast, production of GM-CSF in LN cells was not affected even at the highest IQ-1S dose tested

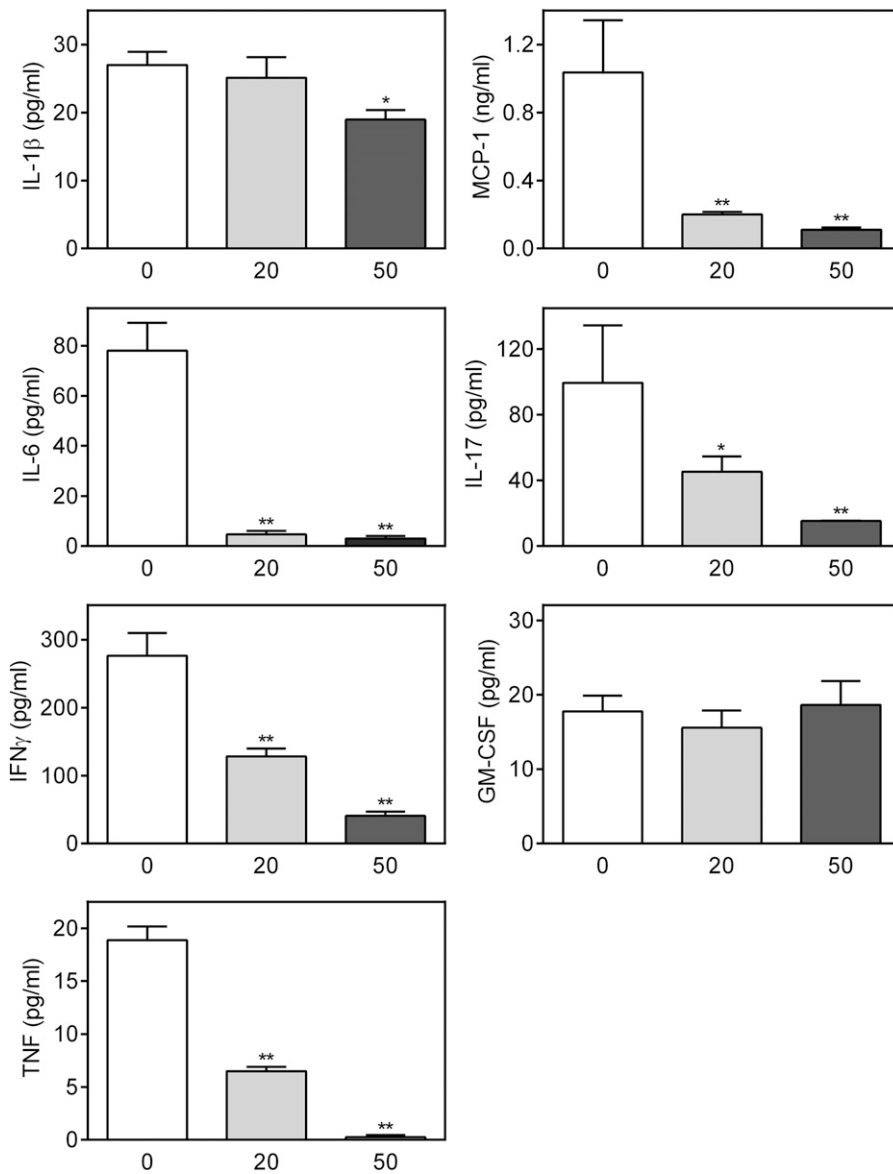


Fig. 8. Effect of IQ-1S on cytokine production by LN cells. Starting at day 7 after the CII challenge, mice were treated intraperitoneally daily with saline (0), 20 mg/kg IQ-1S (20), or 50 mg/kg IQ-1S (50) until day 38. Mice were euthanized, and their LN mononuclear cells were purified and cultured for 3 days with CII. Cytokine levels were measured in supernatants by ELISA. The results show the mean of one experiment (three to four replicates) \pm S.D., which is representative of three independent experiments. * $P < 0.05$; ** $P < 0.01$ compared with saline control.

(50 mg/kg). Further studies are clearly required to define the cell-type sensitivity and/or tissue bioavailability of the inhibitor.

In RA, macrophages and FLSs infiltrate the synovium and secrete proinflammatory cytokines and MMPs that potentiate and maintain inflammation (Kinne et al., 2000; Davignon et al., 2013). The main cytokines that are required for induction of arthritis in autoimmune models include IL-1 β , IL-6, IL-17, TNF, and GM-CSF (Nakae et al., 2003; Guma et al., 2010; Li et al., 2012). JNK1 controls IL-1 β production by mast cells in inflammatory arthritis (Guma et al., 2010), and IL-1 β plays important roles in inflammation and destruction in synovial tissue, cartilage, bone, and joints in patients with RA (Tak and Bresnihan, 2000). TNF, mainly produced by macrophages, can amplify the inflammatory cascade in RA, and five TNF inhibitors are currently approved for treatment of immune-mediated inflammatory diseases, including RA (Armuzzi et al., 2014). Both IL-1 β and TNF induce synoviolin, an E3 ubiquitin ligase expressed in synovial fibroblasts, which is involved in the overgrowth of synovial cells during RA (Gao et al., 2006). IL-6 promotes joint inflammation and cartilage destruction in

various forms of arthritis, and elevated IL-6 and TNF levels were found in synovial fluid and serum from patients with RA (van Leeuwen et al., 1995). Similar to our findings, therapeutic effects of some small-molecule kinase inhibitors in animal models of RA were accompanied by significantly reduced cytokine levels in the paw tissue or ankle joints. For example, IL-1 β , IL-6, TNF, and IFN- γ were significantly reduced in the paw tissue of CIA mice treated with TPCA-1 (2-[(aminocarbonyl)amino]-5-(4-fluorophenyl)-3-thiophenecarboxamide), a selective inhibitor of IKK-2 (Podolin et al., 2005). Administration of another IKK inhibitor BMS-345541 [4-(2'-aminoethyl)amino-1,8-dimethylimidazo[1,2-*a*]quinoxaline] decreased IL-1 β levels in the joints of CIA mice (McIntyre et al., 2003). Likewise, FR167653 [1-(7-(4-fluorophenyl)-1,2,3,4-tetrahydro-8-(4-pyridyl)pyrazolo[5,1-*c*](1,2,4)triazin-2-yl)-2-phenylethanedione sulfate monohydrate], a potent p38 MAPK inhibitor, lowered IL-1 β concentrations in ankle joints of CIA rats (Nishikawa et al., 2003).

JNKs play multiple roles in T-cell activation, differentiation, and cytokine production (reviewed in Rincón and Pedraza-Alva,

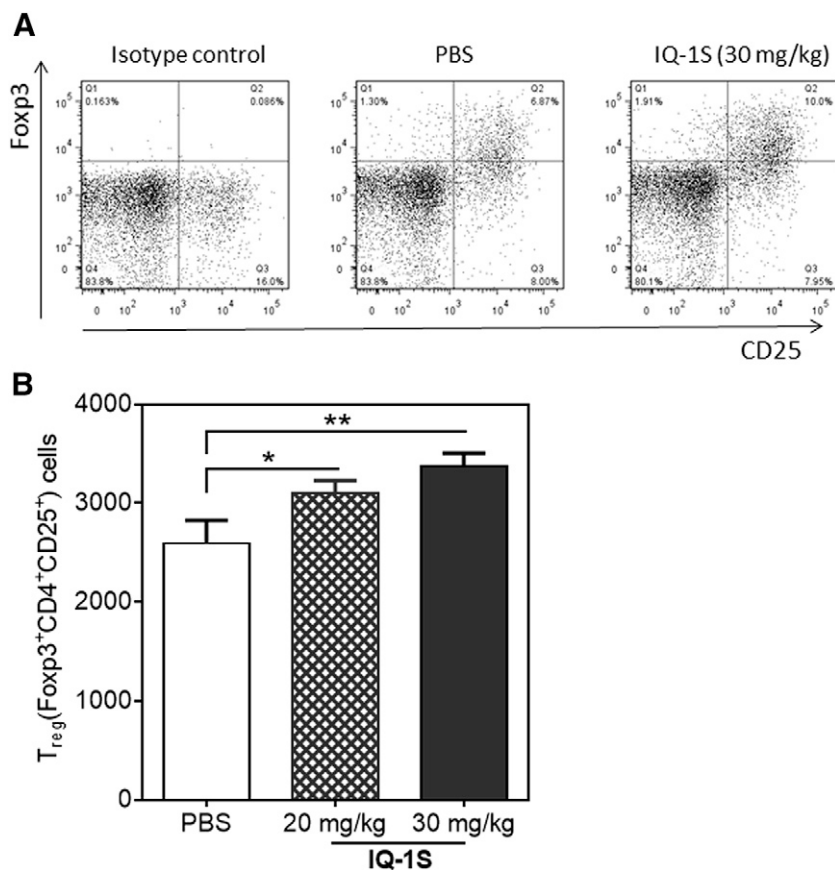


Fig. 9. Effect of IQ-1S on number of Tregs. Starting at day 7 after the CII challenge, mice were treated intraperitoneally daily with saline, 20 mg/kg IQ-1S, or 30 mg/kg IQ-1S until day 38. Mice were euthanized, LNs were collected, and the total number of LN CD4⁺CD25⁺Foxp3⁺ T cells was determined by flow cytometry. (A) Representative flow cytometry plots of gated CD4⁺ T cells from LNs of saline-treated or IQ-1S-treated mice (30 mg/kg). Pooled LN cells were stained for CD4, CD25, and Foxp3. Anti-Foxp3 isotype control cells are shown in the left panel. (B) Evaluation of CD4⁺CD25⁺Foxp3⁺ T cells in IQ-1S-treated and control mice. The results show the mean of one experiment (four replicates) \pm S.D., which is representative of three independent experiments. * $P < 0.05$; ** $P < 0.01$ compared with saline control. PBS, phosphate-buffered saline.

2003; Karin and Gallagher, 2005; Rincón and Davis, 2009). Moreover, the JNK pathway plays a central role in Treg functions, with therapeutic implications for the treatment of autoimmune diseases (Joetham et al., 2012; Wachstein et al., 2012; Chen et al., 2013). Natural Tregs mediate their suppression by inhibiting cytokine responses and inflammatory cell proliferation in an antigen-dependent and -independent fashion (Campbell and Ziegler, 2007). Although there are many Treg subsets, including CD25⁻ cells (Lehmann et al., 2002), CD25⁺CD4⁺Foxp3⁺ natural Tregs are the main subset responsible for suppressing the development of autoreactive T cells (Campbell and Ziegler, 2007). In this study, we show that treatment of CIA mice with IQ-1S dose-dependently increased the number of natural Tregs. The JNK pathway was recently reported to play a central modulatory role in Treg function. Depending on the modulator, JNK inhibition can positively or negatively affect the immunosuppressed function of these cells. For example, exposure of Tregs to JNK inhibitor reduced the immunosuppressive function of heat shock protein 70-treated Tregs (Wachstein et al., 2012). However, incubation of glucocorticoid-induced tumor necrosis receptor ligand-stimulated Tregs with JNK inhibitor SP600125 resulted in the restoration of Treg suppressor activity (Joetham et al., 2012). Suppressor activity of sorted Tregs from CIA mice was previously demonstrated in T-cell proliferation assays using the same conditions and CIA protocol as described here (Kochetkova et al., 2010). Although we did not evaluate the effect of IQ-1S on functional activity of Tregs, our results rule out a total immunosuppressive effect by this compound and suggest complex immunomodulation. Nevertheless, further studies will be necessary in the future to fully evaluate this issue.

Although our previous and current studies clearly demonstrate that IQ-1S inhibits JNKs, additional unrelated mechanisms of action have not been fully excluded to explain its antiarthritic properties, and compounds with structural similarities to IQ-1S have been reported to have a number of biologic activities. For example, several *N*-(1*H*-indeno[1,2-*b*]quinoxalin-11-ylidene)benzohydrazide derivatives with structures related to IQ-1S were recently reported as α -glucosidase inhibitors (Khan et al., 2014), and other structurally unrelated α -glucosidase inhibitors have been reported to have immunosuppressive and immunomodulatory properties (Willenborg et al., 1992; van den Broek et al., 1996). The indeno[1,2-*b*]quinoxaline nucleus of IQ-1S is a flat aromatic ring structure (Ghalib et al., 2010), and planar fused heterocyclic compounds can exhibit a wide variety of pharmacological activities, including DNA intercalation and inhibition of topoisomerases *III* (Deady et al., 1997; Moorthy et al., 2013). Although we did not evaluate potential DNA-intercalating and topoisomerase-inhibiting properties of IQ-1S, this compound was noncytotoxic at high concentrations (Schepetkin et al., 2012), whereas many DNA intercalators (e.g., ellipticine) and topoisomerase inhibitors are cytotoxic (Cros et al., 1975). On the other hand, further development of ellipticine analogs led to the synthesis of DNA-intercalating agents with antiviral, cytotoxic, and immunomodulatory properties, including compound B220 [2,3-dimethyl-6-(2-dimethylaminoethyl)-6*H*-indolo-(2,3-*b*)quinoxaline] and Rabeximod (Harbecke et al., 1999; Hultqvist et al., 2009). Although the IQ-1S structure is similar to Rabeximod and compound B220 (i.e., all three contain isomorphous tetracyclic moieties with a pyrazine cycle), we found that the plane of the Rabeximod heterocyclic moiety

was orientated quite differently from that of SP600125 and IQ-1S, and it did not dock well into the JNK1 binding site and was not positioned to interact with key JNK1 residues, suggesting that it is likely not a JNK inhibitor. Clearly, further work is important to evaluate additional JNK off-target anti-inflammatory and immunomodulatory mechanisms of IQ-1S and its analogs.

In conclusion, we demonstrated that the pan-JNK inhibitor IQ-1S has beneficial anti-inflammatory properties and potentially represents a class of therapeutic agents for development in treatment of RA. IQ-1S also represents an effective small-molecule modulator for mechanistic studies of JNK function in autoimmune arthritis.

Authorship Contributions

Participated in research design: Schepetkin, Kirpotina, Hammaker, Kochetkova, Khlebnikov, Lyakhov, Firestein, Quinn.

Conducted experiments: Schepetkin, Kirpotina, Hammaker, Khlebnikov, Lyakhov.

Contributed new reagents or analytic tools: Schepetkin, Lyakhov.

Performed data analysis: Schepetkin, Kirpotina, Hammaker, Kochetkova, Khlebnikov, Lyakhov, Firestein, Quinn.

Wrote or contributed to the writing of the manuscript: Schepetkin, Hammaker, Kochetkova, Khlebnikov, Lyakhov, Firestein, Quinn.

References

- Albert AS and Serjeant EP (1984) Determination of ionization constants by spectrophotometry, in *The Determination of Ionization Constants*, pp 70–101, Springer, Dordrecht, The Netherlands.
- Alvaro-Gracia JM, Zvaifler NJ, and Firestein GS (1990) Cytokines in chronic inflammatory arthritis. V. Mutual antagonism between interferon-gamma and tumor necrosis factor-alpha on HLA-DR expression, proliferation, collagenase production, and granulocyte macrophage colony-stimulating factor production by rheumatoid arthritis synoviocytes. *J Clin Invest* **86**:1790–1798.
- Armuzzi A, Lionetti P, Blandizzi C, Caporali R, Chimenti S, Cimino L, Gionchetti P, Girolomoni G, Lapadula G, Marchesoni A, et al. (2014) Anti-TNF agents as therapeutic choice in immune-mediated inflammatory diseases: focus on adalimumab. *Int J Immunopathol Pharmacol* **27** (Suppl)11–32.
- Arnett FC, Edworthy SM, Bloch DA, McShane DJ, Fries JF, Cooper NS, Healey LA, Kaplan SR, Liang MH, Luthra HS, et al. (1988) The American Rheumatism Association 1987 revised criteria for the classification of rheumatoid arthritis. *Arthritis Rheum* **31**:315–324.
- Azizi G, Jadidi-Niaragh F, and Mirshafiey A (2013) Th17 cells in immunopathogenesis and treatment of rheumatoid arthritis. *Int J Rheum Dis* **16**:243–253.
- Bain J, McLaughlan H, Elliott M, and Cohen P (2003) The specificities of protein kinase inhibitors: an update. *Biochem J* **371**:199–204.
- Bartok B and Firestein GS (2010) Fibroblast-like synoviocytes: key effector cells in rheumatoid arthritis. *Immunol Rev* **233**:233–255.
- Bernotiene E, Palmer G, Talabot-Ayer D, Szalay-Quinodoz I, Aubert ML, and Gabay C (2004) Delayed resolution of acute inflammation during zymosan-induced arthritis in leptin-deficient mice. *Arthritis Res Ther* **6**:R256–R263.
- Bhagwat SS (2007) MAP kinase inhibitors in inflammation and autoimmune disorders. *Annu Rev Med Chem* **42**:265–278.
- Bogoyevitch MA, Boehm I, Oakley A, Ketterman AJ, and Barr RK (2004) Targeting the JNK MAPK cascade for inhibition: basic science and therapeutic potential. *Biochim Biophys Acta* **1697**:89–101.
- Bogoyevitch MA, Ngoei KR, Zhao TT, Yeap YY, and Ng DC (2010) c-Jun N-terminal kinase (JNK) signaling: recent advances and challenges. *Biochim Biophys Acta* **1804**:463–475.
- Brand DD, Kang AH, and Rosloniec EF (2003) Immunopathogenesis of collagen arthritis. *Springer Semin Immunopathol* **25**:3–18.
- Burrage PS, Mix KS, and Brinckerhoff CE (2006) Matrix metalloproteinases: role in arthritis. *Front Biosci* **11**:529–543.
- Campbell DJ and Ziegler SF (2007) FOXP3 modifies the phenotypic and functional properties of regulatory T cells. *Nat Rev Immunol* **7**:305–310.
- Cao Y, Takada E, Hata K, Sudo K, Furuhashi M, and Mizuguchi J (2010) Enhanced T cell-independent antibody responses in c-Jun N-terminal kinase 2 (JNK2)-deficient B cells following stimulation with CpG-1826 and anti-IgM. *Immunol Lett* **132**:38–44.
- Carranza F, Falcón CR, Nuñez N, Knubel C, Correa SG, Bianco I, Maccioni M, Fretes R, Triquell MF, Motrán CC, et al. (2012) Helminth antigens enable CpG-activated dendritic cells to inhibit the symptoms of collagen-induced arthritis through Foxp3+ regulatory T cells. *PLoS ONE* **7**:e40356.
- Chen L, Wu J, Ren W, Yang X, and Shen Z (2013) c-Jun N-terminal kinase (JNK)-phospho-c-JUN (ser63/73) pathway is essential for FOXP3 nuclear translocation in psoriasis. *J Dermatol Sci* **69**:114–121.
- Coffey G, DeGuzman F, Inagaki M, Pak Y, Delaney SM, Ives D, Betz A, Jia ZJ, Pandey A, Baker D, et al. (2012) Specific inhibition of spleen tyrosine kinase suppresses leukocyte immune function and inflammation in animal models of rheumatoid arthritis. *J Pharmacol Exp Ther* **340**:350–359.
- Cohen S and Fleischmann R (2010) Kinase inhibitors: a new approach to rheumatoid arthritis treatment. *Curr Opin Rheumatol* **22**:330–335.
- Cros J, Thibault A, and Dat-Xuong N (1975) [Anti-inflammatory effect of hydroxy-9-ellipticine]. *C R Acad Sci Hebd Seances Acad Sci D* **281**:1139–1142.
- Cuzzocrea S, Mazzon E, Di Paola R, Muià C, Crisafulli C, Dugo L, Collin M, Britti D, Caputi AP, and Thiemermann C (2006) Glycogen synthase kinase-3beta inhibition attenuates the degree of arthritis caused by type II collagen in the mouse. *Clin Immunol* **120**:57–67.
- Davignon JL, Hayder M, Baron M, Boyer JF, Constantin A, Apparailly F, Poupot R, and Cantagrel A (2013) Targeting monocytes/macrophages in the treatment of rheumatoid arthritis. *Rheumatology (Oxford)* **52**:590–598.
- Deady LW, Kaye AJ, Finlay GJ, Baguley BC, and Denny WA (1997) Synthesis and antitumor properties of N-[2-(dimethylamino)ethyl]carboxamide derivatives of fused tetracyclic quinolines and quinoxalines: a new class of putative topoisomerase inhibitors. *J Med Chem* **40**:2040–2046.
- Dehlin M, Andersson S, Erlandsson M, Brisslert M, and Bokarewa M (2011) Inhibition of fms-like tyrosine kinase 3 alleviates experimental arthritis by reducing formation of dendritic cells and antigen presentation. *J Leukoc Biol* **90**:811–817.
- Dérjard B, Hibi M, Wu IH, Barrett T, Su B, Deng T, Karin M, and Davis RJ (1994) JNK1: a protein kinase stimulated by UV light and Ha-Ras that binds and phosphorylates the c-Jun activation domain. *Cell* **76**:1025–1037.
- Drexler SK, Kong PL, Wales J, and Foxwell BM (2008) Cell signalling in macrophages, the principal innate immune effector cells of rheumatoid arthritis. *Arthritis Res Ther* **10**:216.
- Fabian MA, Biggs WH, 3rd, Treiber DK, Atteridge CE, Azimioara MD, Benedetti MG, Carter TA, Ciceri P, Edeen PT, Floyd M, et al. (2005) A small molecule-kinase interaction map for clinical kinase inhibitors. *Nat Biotechnol* **23**:329–336.
- Firestein GS (2003) Evolving concepts of rheumatoid arthritis. *Nature* **423**:356–361.
- Gao B, Calhoun K, and Fang D (2006) The proinflammatory cytokines IL-1beta and TNF-alpha induce the expression of Synoviolin, an E3 ubiquitin ligase, in mouse synovial fibroblasts via the Erk1/2-ETS1 pathway. *Arthritis Res Ther* **8**:R172.
- Ghalib RM, Hashim R, Sulaiman O, Hemamalini M, and Fun HK (2010) 11H-Indeno-[1,2-b]quinoxalin-11-one. *Acta Crystallogr Sect E Struct Rep Online* **66**:o1494.
- Guma M and Firestein GS (2012) c-Jun N-terminal kinase in inflammation and rheumatic diseases. *Open Rheumatol J* **6**:220–231.
- Guma M, Kashiwakura J, Crain B, Kawakami Y, Beutler B, Firestein GS, Kawakami T, Karin M, and Corr M (2010) JNK1 controls mast cell degranulation and IL-1beta production in inflammatory arthritis. *Proc Natl Acad Sci USA* **107**:22122–22127.
- Guma M, Ronacher LM, Firestein GS, Karin M, and Corr M (2011) JNK-1 deficiency limits macrophage-mediated antigen-induced arthritis. *Arthritis Rheum* **63**:1603–1612.
- Gupta S, Barrett T, Whitmarsh AJ, Cavanagh J, Sluss HK, Dérjard B, and Davis RJ (1996) Selective interaction of JNK protein kinase isoforms with transcription factors. *EMBO J* **15**:2760–2770.
- Han H, Lee KS, Rong W, and Zhang G (2012) Different roles of peripheral mitogen-activated protein kinases in carrageenan-induced arthritic pain and arthritis in rats. *Anesth Analg* **115**:1221–1227.
- Han Z, Boyle DL, Aupperle KR, Bennett B, Manning AM, and Firestein GS (1999) Jun N-terminal kinase in rheumatoid arthritis. *J Pharmacol Exp Ther* **291**:124–130.
- Han Z, Boyle DL, Chang L, Bennett B, Karin M, Yang L, Manning AM, and Firestein GS (2001) c-Jun N-terminal kinase is required for metalloproteinase expression and joint destruction in inflammatory arthritis. *J Clin Invest* **108**:73–81.
- Harbecke O, Dahlgren C, Bergman J, and Möller L (1999) The synthetic non-toxic drug 2,3-dimethyl-6-(2-dimethylaminoethyl)-6H-indolo-(2,3-b)quinoxaline inhibits neutrophil production of reactive oxygen species. *J Leukoc Biol* **65**:771–777.
- Hegen M, Keith JC, Jr, Collins M, and Nickerson-Nutter CL (2008) Utility of animal models for identification of potential therapeutics for rheumatoid arthritis. *Ann Rheum Dis* **67**:1505–1515.
- Heo YS, Kim SK, Seo CI, Kim YK, Sung BJ, Lee HS, Lee JI, Park SY, Kim JH, Hwang KY, et al. (2004) Structural basis for the selective inhibition of JNK1 by the scaffolding protein JIP1 and SP600125. *EMBO J* **23**:2185–2195.
- Hultqvist M, Nandakumar KS, Björklund U, and Holmdahl R (2009) The novel small molecule drug Rabeximod is effective in reducing disease severity of mouse models of autoimmune disorders. *Ann Rheum Dis* **68**:130–135.
- Inoue T, Hammaker D, Boyle DL, and Firestein GS (2005) Regulation of p38 MAPK by MAPK kinases 3 and 6 in fibroblast-like synoviocytes. *J Immunol* **174**:4301–4306.
- Inoue T, Hammaker D, Boyle DL, and Firestein GS (2006) Regulation of JNK by MKK-7 in fibroblast-like synoviocytes. *Arthritis Rheum* **54**:2127–2135.
- Joetham A, Ohnishi H, Okamoto M, Takeda K, Schedel M, Domenico J, Dakhama A, and Gelfand EW (2012) Loss of T regulatory cell suppression following signaling through glucocorticoid-induced tumor necrosis receptor (GITR) is dependent on c-Jun N-terminal kinase activation. *J Biol Chem* **287**:17100–17108.
- Karaman MW, Herrgard S, Treiber DK, Gallant P, Atteridge CE, Campbell BT, Chan KW, Ciceri P, Davis MI, Edeen PT, et al. (2008) A quantitative analysis of kinase inhibitor selectivity. *Nat Biotechnol* **26**:127–132.
- Karin M and Gallagher E (2005) From JNK to pay dirt: jun kinases, their biochemistry, physiology and clinical importance. *IUBMB Life* **57**:283–295.
- Khan MS, Munawar MA, Ashraf M, Alam U, Ata A, Asiri AM, Kousar S, and Khan MA (2014) Synthesis of novel indenoquinoxaline derivatives as potent α -glucosidase inhibitors. *Bioorg Med Chem* **22**:1195–1200.
- Kinne RW, Bräuer R, Stuhlmüller B, Palombo-Kinne E, and Burmester GR (2000) Macrophages in rheumatoid arthritis. *Arthritis Res* **2**:189–202.
- Koch P, Gehring M, and Laufer SA (2015) Inhibitors of c-Jun N-terminal kinases: an update. *J Med Chem* **58**:72–95.
- Kochetkova I, Golden S, Holderness K, Callis G, and Pascual DW (2010) IL-35 stimulation of CD39+ regulatory T cells confers protection against collagen II-induced arthritis via the production of IL-10. *J Immunol* **184**:7144–7153.
- Kochetkova I, Thornburg T, Callis G, Holderness K, Maddaloni M, and Pascual DW (2014) Oral *Escherichia coli* colonization factor antigen I fimbriae ameliorate arthritis via IL-35, not IL-27. *J Immunol* **192**:804–816.

- Kochetkova I, Trunkle T, Callis G, and Pascual DW (2008) Vaccination without autoantigen protects against collagen II-induced arthritis via immune deviation and regulatory T cells. *J Immunol* **181**:2741–2752.
- Köller M, Hayer S, Redlich K, Ricci R, David JP, Steiner G, Smolen JS, Wagner EF, and Schett G (2005) JNK1 is not essential for TNF-mediated joint disease. *Arthritis Res Ther* **7**:R166–R173.
- Kyttaris VC (2012) Kinase inhibitors: a new class of antirheumatic drugs. *Drug Des Devel Ther* **6**:245–250.
- Lee E, Jeong KW, Shin A, Jin B, Jnawali HN, Jun BH, Lee JY, Heo YS, and Kim Y (2013) Binding model for eriodictyol to Jun-N terminal kinase and its anti-inflammatory signaling pathway. *BMB Rep* **46**:594–599.
- Lee SI, Boyle DL, Berdeja A, and Firestein GS (2012) Regulation of inflammatory arthritis by the upstream kinase mitogen activated protein kinase kinase 7 in the c-Jun N-terminal kinase pathway. *Arthritis Res Ther* **14**:R38.
- Lehmann J, Huehn J, de la Rosa M, Maszyra F, Kretschmer U, Krenn V, Brunner M, Scheffold A, and Hamann A (2002) Expression of the integrin alpha Ebeta 7 identifies unique subsets of CD25+ as well as CD25- regulatory T cells. *Proc Natl Acad Sci USA* **99**:13031–13036.
- Li J, Hsu HC, and Mountz JD (2012) Managing macrophages in rheumatoid arthritis by reform or removal. *Curr Rheumatol Rep* **14**:445–454.
- Liacini A, Sylvester J, Li WQ, and Zafarullah M (2002) Inhibition of interleukin-1-stimulated MAP kinases, activating protein-1 (AP-1) and nuclear factor kappa B (NF-kappa B) transcription factors down-regulates matrix metalloproteinase gene expression in articular chondrocytes. *Matrix Biol* **21**:251–262.
- Manning AM and Davis RJ (2003) Targeting JNK for therapeutic benefit: from junk to gold? *Nat Rev Drug Discov* **2**:554–565.
- McIntyre KW, Shuster DJ, Gilooly KM, Dambach DM, Pattoli MA, Lu P, Zhou XD, Qiu Y, Zusi FC, and Burke JR (2003) A highly selective inhibitor of I kappa B kinase, BMS-345541, blocks both joint inflammation and destruction in collagen-induced arthritis in mice. *Arthritis Rheum* **48**:2652–2659.
- Mehan S, Meena H, Sharma D, and Sankhla R (2011) JNK: a stress-activated protein kinase therapeutic strategies and involvement in Alzheimer's and various neurodegenerative abnormalities. *J Mol Neurosci* **43**:376–390.
- Meier FM and McInnes IB (2014) Small-molecule therapeutics in rheumatoid arthritis: scientific rationale, efficacy and safety. *Best Pract Res Clin Rheumatol* **28**:605–624.
- Moorthy NSHN, Manivannan E, Karthikeyan C, and Trivedi P (2013) 6H-Indolo[2,3-b]quinoxalines: DNA and protein interacting scaffold for pharmacological activities. *Mini Rev Med Chem* **13**:1415–1420.
- Myers LK, Rosloniec EF, Cremer MA, and Kang AH (1997) Collagen-induced arthritis, an animal model of autoimmunity. *Life Sci* **61**:1861–1878.
- Nakae S, Nambu A, Sudo K, and Iwakura Y (2003) Suppression of immune induction of collagen-induced arthritis in IL-17-deficient mice. *J Immunol* **171**:6173–6177.
- Nandakumar KS, Andrén M, Martinsson P, Bajtner E, Hellström S, Holmdahl R, and Kleinau S (2003) Induction of arthritis by single monoclonal IgG anti-collagen type II antibodies and enhancement of arthritis in mice lacking inhibitory Fc gammaRIIB. *Eur J Immunol* **33**:2269–2277.
- Nishikawa M, Myoui A, Tomita T, Takahi K, Nampei A, and Yoshikawa H (2003) Prevention of the onset and progression of collagen-induced arthritis in rats by the potent p38 mitogen-activated protein kinase inhibitor FR167653. *Arthritis Rheum* **48**:2670–2681.
- Ogata M, Matsumoto H, Shimizu S, Kida S, Wada T, Shiro M, and Sato K (1986) Synthesis and antiviral activity of sulfonamidobenzophenone oximes and sulfonamidobenzamides. *J Med Chem* **29**:417–423.
- Ohori M, Takeuchi M, Maruki R, Nakajima H, and Miyake H (2007) FR180204, a novel and selective inhibitor of extracellular signal-regulated kinase, ameliorates collagen-induced arthritis in mice. *Naunyn Schmiedeberg's Arch Pharmacol* **374**:311–316.
- Pesu M, Laurence A, Kishore N, Zwillich SH, Chan G, and O'Shea JJ (2008) Therapeutic targeting of Janus kinases. *Immunol Rev* **223**:132–142.
- Podolin PL, Callahan JF, Bolognese BJ, Li YH, Carlson K, Davis TG, Mellor GW, Evans C, and Roshak AK (2005) Attenuation of murine collagen-induced arthritis by a novel, potent, selective small molecule inhibitor of I kappa B kinase 2, TPCA-1 (2-[aminocarbonyl]amino]-5-(4-fluorophenyl)-3-thiophenecarboxamide), occurs via reduction of proinflammatory cytokines and antigen-induced T cell proliferation. *J Pharmacol Exp Ther* **312**:373–381.
- Prince HE (2005) Biomarkers for diagnosing and monitoring autoimmune diseases. *Biomarkers* **10** (Suppl 1):S44–S49.
- Rincón M and Davis RJ (2009) Regulation of the immune response by stress-activated protein kinases. *Immunol Rev* **228**:212–224.
- Rincón M and Pedraza-Alva G (2003) JNK and p38 MAP kinases in CD4+ and CD8+ T cells. *Immunol Rev* **192**:131–142.
- Rosengren S, Corr M, Firestein GS, and Boyle DL (2012) The JAK inhibitor CP-690,550 (tofacitinib) inhibits TNF-induced chemokine expression in fibroblast-like synoviocytes: autocrine role of type I interferon. *Ann Rheum Dis* **71**:440–447.
- Schepetkin IA, Kirpotina LN, Khlebnikov AI, Hanks TS, Kochetkova I, Pascual DW, Julita MA, and Quinn MT (2012) Identification and characterization of a novel class of c-Jun N-terminal kinase inhibitors. *Mol Pharmacol* **81**:832–845.
- Schramm C, Kriegsmann J, Protschka M, Huber S, Hansen T, Schmitt E, Galle PR, and Blessing M (2004) Susceptibility to collagen-induced arthritis is modulated by TGFbeta responsiveness of T cells. *Arthritis Res Ther* **6**:R114–R119.
- Schurgers E, Billiau A, and Matthys P (2011) Collagen-induced arthritis as an animal model for rheumatoid arthritis: focus on interferon-gamma. *J Interferon Cytokine Res* **31**:917–926.
- Stevens TL, Bossie A, Sanders VM, Fernandez-Botran R, Coffman RL, Mosmann TR, and Vitetta ES (1988) Regulation of antibody isotype secretion by subsets of antigen-specific helper T cells. *Nature* **334**:255–258.
- Sundarrajan M, Boyle DL, Chabaud-Riou M, Hammaker D, and Firestein GS (2003) Expression of the MAPK kinases MKK-4 and MKK-7 in rheumatoid arthritis and their role as key regulators of JNK. *Arthritis Rheum* **48**:2450–2460.
- Tak PP and Bresnihan B (2000) The pathogenesis and prevention of joint damage in rheumatoid arthritis: advances from synovial biopsy and tissue analysis. *Arthritis Rheum* **43**:2619–2633.
- Thalhamer T, McGrath MA, and Harnett MM (2008) MAPKs and their relevance to arthritis and inflammation. *Rheumatology (Oxford)* **47**:409–414.
- Tissi L, Bistoni F, and Puliti M (2009) IL-4 deficiency decreases mortality but increases severity of arthritis in experimental group B Streptococcus infection. *Mediators Inflamm* **2009**:394021.
- Toyama S, Tamura N, Haruta K, Karakida T, Mori S, Watanabe T, Yamori T, and Takasaki Y (2010) Inhibitory effects of ZSTK474, a novel phosphoinositide 3-kinase inhibitor, on osteoclasts and collagen-induced arthritis in mice. *Arthritis Res Ther* **12**:R92.
- Triantaphyllopoulos K, Madden L, Rioja I, Essex D, Buckton J, Malhotra R, Ray K, Binks M, and Paleolog EM (2010) In vitro target validation and in vivo efficacy of p38 MAP kinase inhibition in established chronic collagen-induced arthritis model: a pre-clinical study. *Clin Exp Rheumatol* **28**:176–185.
- van den Broek LAGM, Kat-Van Den Nieuwenhof MW, Butters TD, and Van Boeckel CA (1996) Synthesis of alpha-glucosidase I inhibitors showing antiviral (HIV-1) and immunosuppressive activity. *J Pharm Pharmacol* **48**:172–178.
- van Leeuwen MA, Westra J, Limburg PC, van Riel PL, and van Rijswijk MH (1995) Interleukin-6 in relation to other proinflammatory cytokines, chemotactic activity and neutrophil activation in rheumatoid synovial fluid. *Ann Rheum Dis* **54**:33–38.
- Vinh NB, Simpson JS, Scammells PJ, and Chalmers DK (2012) Virtual screening using a conformationally flexible target protein: models for ligand binding to p38alpha MAPK. *J Comput Aided Mol Des* **26**:409–423.
- Wachstein J, Tischer S, Figueiredo C, Limbourg A, Falk C, Immenschuh S, Blasczyk R, and Eiz-Vesper B (2012) HSP70 enhances immunosuppressive function of CD4 (+)CD25(+)FoxP3(+) T regulatory cells and cytotoxicity in CD4(+)/CD25(-) T cells. *PLoS ONE* **7**:e51747.
- Wang T, Arifoglu P, Ronai Z, and Tew KD (2001) Glutathione S-transferase P1-1 (GSTP1-1) inhibits c-Jun N-terminal kinase (JNK1) signaling through interaction with the C terminus. *J Biol Chem* **276**:20999–21003.
- Willenborg DO, Parish CR, and Cowden WB (1992) Inhibition of adjuvant arthritis in the rat by phosphosugars and the alpha-glucosidase inhibitor castanospermine. *Immunol Cell Biol* **70**:369–377.
- Xu D, Kim Y, Postelnek J, Vu MD, Hu DQ, Liao C, Bradshaw M, Hsu J, Zhang J, Pashine A, et al. (2012) RN486, a selective Bruton's tyrosine kinase inhibitor, abrogates immune hypersensitivity responses and arthritis in rodents. *J Pharmacol Exp Ther* **341**:90–103.
- Zhou CL, Lu R, Lin G, and Yao Z (2011) The latest developments in synthetic peptides with immunoregulatory activities. *Peptides* **32**:408–414.

Address correspondence to: Dr. Mark T. Quinn, Department of Microbiology and Immunology, Montana State University, Molecular Bioscience Bldg., Bozeman, MT 59717. E-mail: mquinn@montana.edu